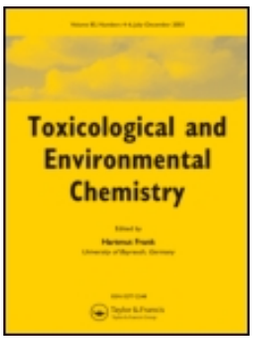

Toxicological & Environmental Chemistry

ISSN: 0277-2248 (Print) 1029-0486 (Online) Journal homepage: http://www.tandfonline.com/loi/gtec20

Application of magnesite–bentonite clay composite as an alternative technology for removal of arsenic from industrial effluents

Vhahangwele Masindi, Mugera W. Gitari, Hlanganani Tutu & Marinda De Beer

To cite this article: Vhahangwele Masindi, Mugera W. Gitari, Hlanganani Tutu & Marinda De Beer (2014) Application of magnesite–bentonite clay composite as an alternative technology for removal of arsenic from industrial effluents, Toxicological & Environmental Chemistry, 96:10, 1435-1451, DOI: 10.1080/02772248.2014.966714

To link to this article: http://dx.doi.org/10.1080/02772248.2014.966714

Toxicological & Environmental Chemistry, 2014
Vol. 96, No. 10, 1435–1451, http://dx.doi.org/10.1080/02772248.2014.966714

Application of magnesite–bentonite clay composite as an alternative technology for removal of arsenic from industrial effluents

Vhahangwele Masindi[a,b]*, Mugera W. Gitari[a], Hlanganani Tutu[c] and Marinda De Beer[d]

[a]*Department of Ecology and Resources Management, University of Venda, Thohoyandou, South Africa;* [b]*CSIR (Council of Scientific and Industrial Research), Built Environment, Building Science and Technology (BST), Pretoria, South Africa;* [c]*Molecular Sciences Institute, School of Chemistry, University of Witwatersrand, Johannesburg, South Africa;* [d]*DST/CSIR National Centre for Nano-Structured Materials, Council of Scientific and Industrial Research, Pretoria, South Africa*

(*Received 3 June 2014; accepted 11 September 2014*)

This study evaluated the feasibility of integrating amorphous magnesite and bentonite clay (composite) as an alternative technology for removing arsenic from industrial effluents. The removal of arsenic from industrial effluents by using magnesite–bentonite clay composite was carried out in batch mode. The effects of equilibration time, adsorbent dosage, adsorbate concentration, and pH on removal of arsenic were investigated. The experiments demonstrated that ≈100% arsenic removal is optimum at 30 minutes of agitation, 2 g of adsorbent dosage (2 g: 100 mL, S/L ratio), and 20 mg L^{-1} of arsenic concentration. The adsorption data fitted well to both Langmuir and Freundlich adsorption models, hence proving monolayer and multilayer adsorption. The kinetic studies revealed that the data fitted better to a pseudo-second-order reaction than to a pseudo-first-order reaction, hence proving chemisorption. At optimized conditions, the composite was able to remove arsenic to below World Health Organization water quality guidelines, hence depicting that the composite is effective and efficient in removing arsenic from contaminated water. Based on that, this comparative study proves that the composite is a promising adsorbent with high adsorption capacity for arsenic and can be a suitable substitute for the conventional treatment methods.

Keywords: wastewater; arsenic; magnesite; bentonite clay; batch experiment; composite

Introduction

Availability of arsenic (As) in the biosphere is mainly through anthropogenic activities and geochemical environment (Zachara et al. 1998; Bruce and Goldberg 1996; Misheal and Bleiman 2010; Goh et al. 2010; Lo, Yin, and Tang 2011; Yang, Park, and Lee 2011; Masindi 2012; Aroke, El-Nafaty, and Osha 2014). Introduction of arsenic to surface and subsurface water has been regarded as a problematic issue in recent years due to their toxicity on exposure to terrestrial and aquatic organisms (Alloways 1995; Sparks 1997; Langmuir 1997; WHO 2006; Ramesh et al. 2007; Singh and Bhati 2012). Mobility, distribution, bioavailability, toxicity, bioaccumulation, biodegradability, and transformation (speciation) of arsenic in aqueous environment are governed by its total concentration, redox reaction, pH of the solution, and the geochemistry of the surrounding lithology (Alloways 1995; Sparks 1997; Chien et al. 2012). Drinking water mainly comes from surface and underground water reserves though elevated concentrations of arsenic are

*Corresponding author. Email: vmasindi@csir.co.za

encountered in underground water resources due to weathering of rocks and dissolution (Brammer and Ravenscroft 2009). World Health Organization (WHO) (2006) and Department of Water Affairs and Forestry (DWAF) (1996) recommended 0.01 mg L^{-1} for arsenic in drinking water. Excess availability and long-term exposure to arsenic may lead to the development of various diseases such as conjunctivitis, hyperkeratosis, hyperpigmentation, cardiovascular diseases, disorders of the central nervous system and peripheral vascular system, skin cancer, and gangrene of the limbs (Brammer and Ravenscroft 2009; Khan et al. 2009; Bates, Smith, and Rich 1992; Ramesh et al. 2007; Masindi 2012). Epidemiological studies also reported that excess exposure to the aforementioned chemical species may interfere with metabolic activities of living organisms; consumption of those chemicals may also accelerate multisystem organ failure by allosteric inhibition of sulfhydryl enzymes that are essential for regulating metabolic activities, hence leading to death (Tseng 1977; Chien et al. 2012; Masindi 2012). As such, arsenic needs to be contained and treated prior to contamination of drinking water. Bentonite clay has been applied for adsorption of anionic (As, B, Cr, Mo, and Se) and cationic (Al, Fe, Mn, etc.) species (Masindi 2012; Gitari 2014). Mainly, it scavenges chemical species from aqueous media via precipitation, ion exchange, and adsorption (Sparks 1997). Magnesite is a carbonate mineral that adds alkalinity to a solution (Langmuir 1997). Blending magnesite with bentonite clay will basically add alkalinity to wastewater, hence creating conditions that are suitable for anionic arsenic to react with positively charged surfaces on aqueous solution and suspended chemicals (Langmuir 1997; Sparks 1997). Several technologies have been developed for decontamination of polluted water bodies. However, cost factor, treatment inefficiencies, implementation inconveniencies, and materials availability limit their applications (Masindi 2012). This study, therefore, attempts to evaluate the feasibility of combining magnesite and bentonite clay as an integrated water treatment technology for removal of arsenic species from contaminated and wastewaters. Combination of magnesite and bentonite clay (composite) will increase the concentration of base cations that are suitable for arsenic adsorption, especially at basic conditions (Alloways 1995; Langmuir 1997). Recent studies have reported that the Yellow Star Quarries in the Kroonstad district, Cape Town, Republic of South Africa (RSA), contains 750,000 m^3 deposit of bentonite that can be projected to 67 years if it is mined at a rate of 4000 m^3/month (Masindi 2014; Gitari 2014). The magnesite mine in Folovhodwe, Limpopo province, RSA, showed that the magnesite deposit is close to 18 mega tons of cryptocrystalline magnesite which can be mined for the next 50 years (Agnello 2003). In terms of economic viability, the technology will be feasible since it is relying on natural and locally available materials. The objective of this paper is to evaluate optimum conditions for removal of arsenic from industrial effluent using magnesite–bentonite clay composite.

Experimental

Sampling and preparation of the adsorbent

Magnesite was collected from the Folovhodwe Magnesite mine in Mutale district, Limpopo province, RSA. Bentonite clay was collected from the Yellow Star Quarries in the Kroonstad district, Cape Town, RSA. Raw bentonite clay was washed by soaking the samples in ultrapure water and draining the water after 10 minutes. The procedure was repeated four times. The washed bentonite was then dried in an oven for 24 hours at 105 °C. The magnesite and bentonite clay were milled into fine powder using Retsch model RS 200 miller and passed through a 32-μm-particle-size sieve. The magnesite and

bentonite clay composite was fabricated by mixing magnesite and bentonite clay at 1:1 S/S ratios.

Physiochemical characterization of the adsorbent

Elemental analysis of the water samples was done by inductively coupled plasma mass spectrometry (ICP-MS, ELAN 6000). The accuracy of the analysis was monitored by analysis of National Institute of Standard and Technology (NIST) water standards. Chemical characteristics of magnesite samples were ascertained using X-ray flourescence spectroscopy (XRF). Mineralogical characteristics of magnesite samples were ascertained using a Philips X-ray diffractometer with Cu-Kα radiation. Phase identification was performed by searching and matching the obtained spectra with the powder diffraction file database with the help of JCPDS (Joint Committee of Powder Diffraction Standards) files for inorganic compounds. (Both XRF and XRD (X-ray diffraction) analyses were done at the Department of Geology, University of Pretoria.) Morphology and elemental composition of magnesite were determined by energy dispersive X-ray spectrometry (EDS: FIB-SEM, Auriga from Carl Zeiss) attached to a scanning electron microscopy (SEM: JEOL JSM7500 microscope from Carl Zeiss) (SEM-EDS), and the surface area was estimated by Brunauer–Emmett–Teller analysis (BET: A Tristar II 3020, Micrometrics BET from Norcross, GA, USA). pH_{pzc} was determined using solid addition method as described by Kumar et al. (2011). The cation exchange capacity (CEC) was determined using the ammonium acetate method (Gitari 2014).

Preparation of stock solution

A standard solution of 1000 mg L^{-1}arsenic from Lab Consumables Supply, South Africa, was used to prepare the working solutions. From 1000 mg L^{-1} stock solution, 10 mg L^{-1} solution was prepared by extracting 10 mL of the 1000 mg L^{-1} standard solution and transferring into a 1000 mL volumetric flask. The volumetric flask was topped to the mark by adding ultrapure water.

Batch adsorption studies

Removal of arsenic as a function of time

Eight 100 mL samples of 10 mg L^{-1}arsenic solution were pipetted into eight 250 mL bottles and 1 g of the composite was added. The mixture was then agitated for 1, 5, 10, 15, 30, 60, 180, and 360 minutes at 250 rpm using the Stuart reciprocating shaker. After equilibration, the mixtures were filtered through 0.45 μm pore nitrate cellulose membrane and acidified with two drops of concentrated HNO_3. The samples were refrigerated at 4 °C until analysis by ICP-MS (ELAN 6000).

Removal of arsenic as a function of dosage

Seven 100 mL solutions of 10 mg L^{-1}arsenic solution were pipetted into seven 250 mL bottles and varying masses of the composite were added. The masses of the composite were 0.1, 0.3, 0.5, 1, 2, 3, 4, and 5 g. The mixtures were agitated for 30 minutes at 250 rpm using the Stuart reciprocating shaker. After equilibration, the mixtures were filtered through a 0.45 μm pore nitrate cellulose membrane and acidified with two drops of concentrated HNO_3. The samples were refrigerated at 4 °C until analysis by ICP-MS (ELAN 6000).

Removal of arsenic as a function of concentration

A standard solution of 1000 mg L^{-1}arsenic was used to prepare 0.3, 0.6, 1.25, 5, 10, 20, and 40 mg L^{-1} solutions. Thereafter, 100 mL of the solutions were pipetted into seven 250 mL bottles and 1 g of the composite was added. The mixtures were then agitated for 30 minutes at 250 rpm using the Stuart reciprocating shaker. After equilibration, the mixtures were filtered through a 0.45 μm pore nitrate cellulose membrane and acidified with two drops of concentrated HNO_3. The samples were refrigerated at 4 °C until analysis by ICP-MS (ELAN 6000).

Removal of arsenic as a function of pH

Six 100 mL solutions of 10 mg L^{-1}arsenic solutions were pipetted into six 250 mL bottles. The pH of the solutions was adjusted using 0.1 M of NaOH and 0.01 M of H_2SO_4. The pH of the solutions was varied from 2 to 12. One gram of the composite was added in each of the container. The mixtures were agitated for 30 minutes at 250 rpm using the Stuart reciprocating shaker. After equilibration, the mixtures were filtered through a 0.45 μm pore nitrate cellulose membrane and acidified with two drops of concentrated HNO_3. The samples were refrigerated at 4 °C until analysis by ICP-MS (ELAN 6000).

Removal of arsenic at optimized conditions

A 100 mL of arsenic-rich water was transferred into each of the three 250 mL high-density polyethylene (HDPE) bottles and 1 g of the composite was added. The mixtures were equilibrated for 30 minutes at 250 rpm using the Stuart reciprocating shaker. After agitation, the mixtures were filtered through a 0.45 μm pore cellulose membrane.

Modeling of analytical results

Percentage removal

Percentage removal of arsenic from aqueous media was computed using the following equation:

$$\%\ \text{removal} = \left(\frac{(C_i - C_f)}{C_i}\right) \times 100 \tag{1}$$

where C_i = initial arsenic concentration and C_f = equilibrium arsenic concentration. This will show the amount of arsenic adsorbed by the composite from the aqueous solution.

Adsorption capacity

Adsorption capacity of the composite for arsenic adsorption from aqueous media was computed using the following equation:

$$q = \frac{((C_i - C_f)V)}{m} \tag{2}$$

where C_i = initial arsenic concentration and C_f = equilibrium arsenic concentration at equilibrium (mg L^{-1}), V = volume of arsenic solution (L), and m = weight of bentonite clay (adsorbent) in grams. This will show the amount of arsenic adsorbed per gram of the composite.

Adsorption isotherms

The mechanisms and intensity of adsorption were described using two common adsorption models: Langmuir and Freundlich adsorption isotherms; these models describe the adsorption processes on a homogeneous or heterogeneous surface, respectively.

The Langmuir isotherm is valid for monolayer sorption due to a surface with finite number of identical sites, and can be expressed in the following linear form:

$$\frac{Ce}{Qe} = \frac{1}{Qmb} + \frac{Ce}{Qm} \tag{3}$$

where Ce = equilibrium concentration (mg L^{-1}), Qe = amount adsorbed at equilibrium (mg g^{-1}), Qm = Langmuir constant related to adsorption capacity (mg g^{-1}), and b = Langmuir constant related to energy of adsorption (L mg^{-1}).

A plot of Ce vs. Ce/Qe should be linear if the data is described by the Langmuir isotherm. The value of Qm is determined from the slope and the intercept of the plot. It is used to derive the maximum adsorption capacity and b is determined from the original equation and it represents the intensity of adsorption.

The Freundlich adsorption isotherm describes the heterogeneous surface energy by multilayer adsorption and can be expressed in linear form as

$$log\ Qe = \frac{1}{n} log\ C + logKf \tag{4}$$

where Ce = equilibrium concentration (mg L^{-1}), Qe = amount adsorbed at equilibrium (mg g^{-1}), Kf = partition coefficiency (mg g^{-1}), and n = intensity of adsorption.

The linear plot of log Ce vs. log Qe indicates if the data is described by the Freundlich isotherm. The value of Kf implies that the energy of adsorption on a homogeneous surface is independent of surface coverage and n is an adsorption constant that reveals the rate at which adsorption is taking place. These two constants are determined from the slope.

Adsorption kinetics

The pseudo-first-order is a kinetic model described by the following equation:

$$log(q_e - q_t) = log\ q_e - \left(\frac{k}{2.3}\right)t \tag{5}$$

where q_e (mg g^{-1}) is adsorption capacity at equilibrium, q_t (mg g^{-1}) is the adsorption capacity at time t, and K (min^{-1}) is the rate constant of pseudo-first-order reaction. The value of K_1 can be obtained from the slope by plotting t vs. $\log(q_e - q_t)$.

Pseudo-second-order model is applied when the applicability of the first-order kinetics becomes untenable. The equation of pseudo-second-order is expressed as

$$\frac{1}{q_t} = \frac{1}{k_2 q_e} + \left(\frac{1}{q_e}\right)t \tag{6}$$

This equation is applied to obtain K_2, the second-order rate from the plots t vs. t/q_e .

Table 1. Elemental composition (% weight) of bentonite clay, magnesite, and the composite.

% Composition	Bentonite clay	Magnesite	Composite before
SiO_2	66.51	4.76	51.72
Al_2O_3	16.81	0.14	10.37
Fe_2O_3	3.26	0.25	4.44
MnO	0.13	0	0.1
MgO	3.12	91.80	29.43
CaO	1.43	5.59	2.29
Na_2O	1.17	0	0.79
K_2O	0.54	0.003	0.32

Results and discussion

X-ray fluorescence analysis

The elemental composition of bentonite clay, magnesite, and composite is shown in Table 1.

Bentonite clay is mainly composed of Al and Si, hence proving that the material under study is an aluminosilicate. The presence of Fe indicates possible adsorption of Fe during deposition. The presence of MgO, CaO, NaO, and K shows that these are the main exchangeable cations in bentonite clay matrices. Magnesite is dominated by Mg as the major element, hence validating that the material is magnesium based. The synthesized composite is dominated with Al, Mg, and Si, hence showing that the material is a combination of magnesite and clay mineral.

X-ray diffraction analysis

XRD revealed that the composite is enriched with magnesite, montmorillonite, and quartz (Figure 1). Figure 1 shows the mineralogical composition of the fabricated composite.

XRD analysis also showed that magnesite consisted of periclase, brucite, and forsterite as the main mineral phase (Figure 1(a)). Bentonite clay was observed to contain smectite, quartz, plagioclase, calcite, and muscovite (Figure 1(b)). The composite was determined to contain smectite, periclase, quartz, gibbsite, and muscovite, which are the main components of magnesite and bentonite clay (Figure 1(c)). The presence of periclase in the composite will aid in increasing the alkalinity of the solution, hence promoting conditions that are suitable for arsenic adsorption.

Scanning electron microscopy (SEM) and energy dispersive X-ray spectrometry (EDS)

SEM/EDS scanning electron microscope (SEM) images of magnesite, bentonite clay, and the composite were obtained. The elemental composition analysis done by the EDS corroborated the results obtained by XRF (Table 1).

As shown in Figure 2, the EDS results showed the presence of Mg, C, O, Si, and Ca. The morphology by SEM showed the presence of spherical structures. Masindi (2014) has reported that magnesite contains a fraction of crystalline phases and a portion of amorphous phase. The presence of Mg, C, O, Si, and Ca confirms that the material under study is magnesite. Availability of Mg and Ca on the matrices of the composite will also aid in adsorption of arsenic from aqueous medium.

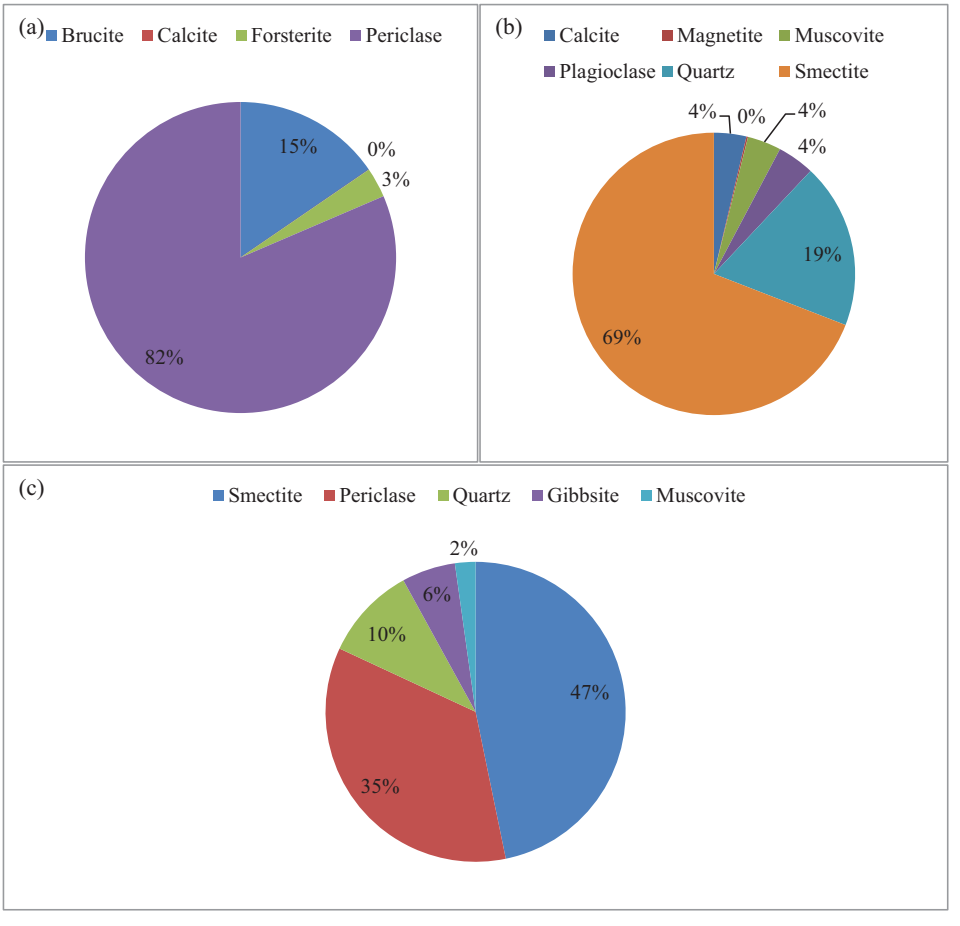

Figure 1. Mineralogical composition of (a) magnesite, (b) bentonite clay, and (c) the composite.

As shown in Figure 3, the EDS results showed the presence of Al, Si, and O as the main constituents, hence the name aluminosilicate. The presence of Mg, Ca, Na, and K shows that these are the exchangeable cations on bentonite clay matrices (Sparks 1997). The morphology by SEM showed the presence of a leafy structure. Impurities of Fe are also present. This might have been adsorbed during deposition and weathering processes. Base cations and Al, Si, and Fe will aid in adsorption of arsenic from aqueous solution.

As shown in Figure 4, the EDS results showed the presence of Al, Si, Mg, and O as the main constituents. This shows that the material under study is a mixture of magnesite and bentonite clay. After modification, the levels of exchangeable cations (particularly Mg) increased significantly, hence indicating higher neutralization potential on the synthesized material. This will play a significant role in creating conditions that are conducive for adsorption of arsenic.

Brunauer–Emmett–Teller (BET) analysis

The surface area of magnesite, bentonite clay, and the composite is presented in Table 2.

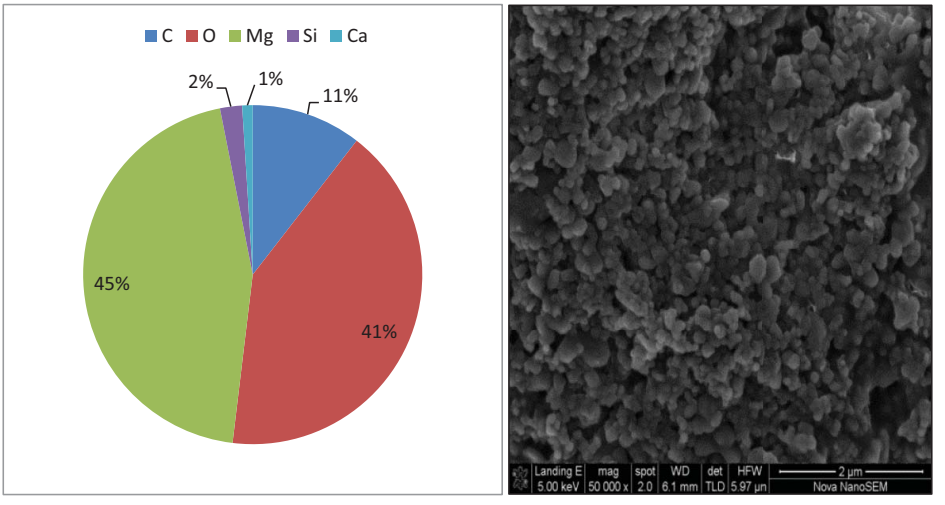

Figure 2. Elemental analysis and SEM image of magnesite.

Surface area is one of the most important aspects of adsorption. If the surface area is high, the adsorption capacity will also be high (Sparks 1997; Masindi 2012). Mixing of magnesite with bentonite clay increases the adsorption surfaces (Table 2) on the fabricated material and this has presented more adsorption sites for arsenic adsorption from arsenic-rich effluents.

Cation exchange capacity

Table 3 shows the CEC of raw bentonite and the composite.

Analysis of CEC by the ammonium acetate method revealed that the main exchangeable cations in the supernatant include Mg^{2+}, Ca^{2+}, Na^{+}, and K^{+}. From the supernatant, it was also observed that Na^{+} is the dominant cation for raw bentonite clay, hence

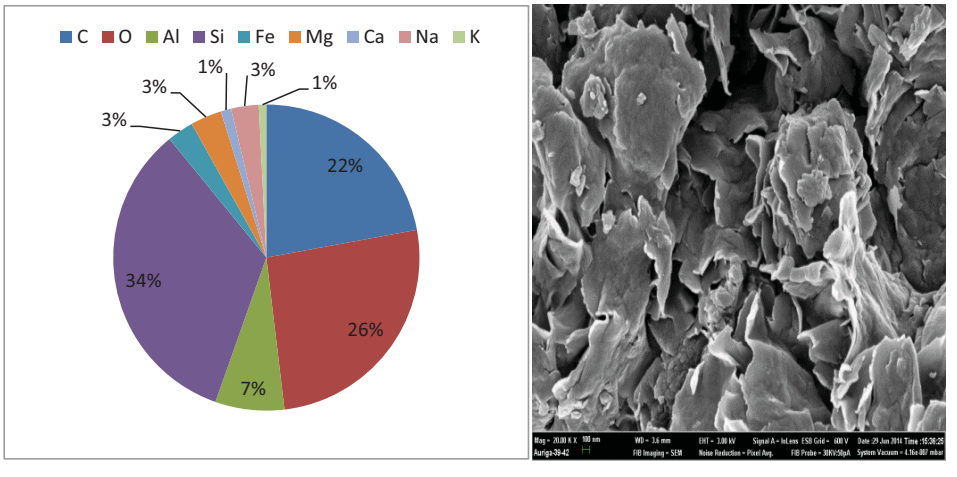

Figure 3. Elemental analysis and SEM image of bentonite clay.

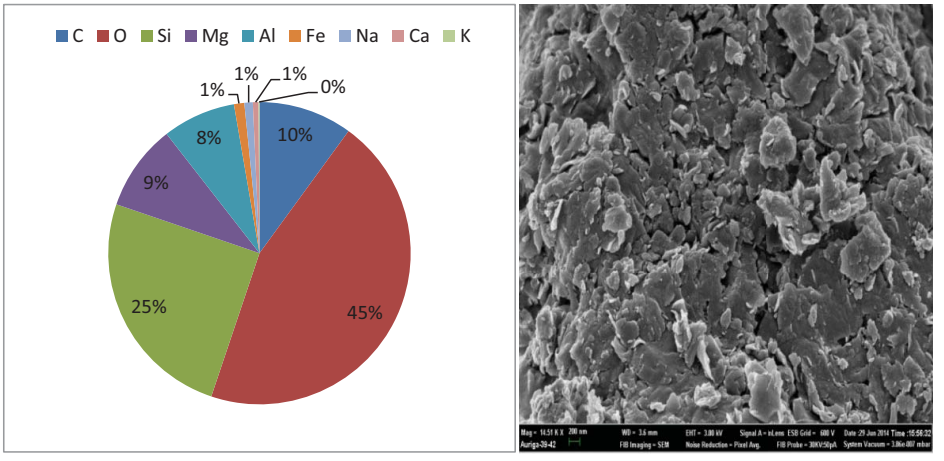

Figure 4. Elemental analysis and SEM image of unreacted composite.

confirming that the clay under study is Na-bentonite. After blending bentonite clay with magnesite, the dominant cation was observed to be Mg^{+}, hence showing that addition of magnesite increases the levels of Mg^{2+} on the composite matrices. Blending of bentonite clay with magnesite increases the CEC of the synthesized composite – this may be attributed to addition of magnesium. Mixing bentonite clay with magnesite led to an increase in the CEC from 262 to 437.1 meq 100 g^{-1} at pH 5.4 and 265.5 to 442.9 meq 100 g^{-1} at pH 7.4. This is a very important aspect of arsenic removal, since those exchangeable cations will aid in adsorption of arsenic from arsenic-rich effluents (Alloways 1995; Langmuir 1997; Sparks 1997).

Point of zero charge (PZC)

Figure 5 (a) and 5(b) shows the pH_{pzc} of bentonite clay and the composite.

Figure 5 (a) and 5(b) shows the initial and change in pH ($\Delta pH = pH_0 - pH_f$) profiles for pH_{pzc} determination. This helps to determine the type of chemical species that will be removed from the aqueous solution. When pH_{pzc} is greater than the supernatant pH, the adsorbent will adsorb cations, and when the pH of the supernatant is above the pH_{pzc}, the adsorbent will adsorb anions from the solution. The study conducted by Sparks (1997) pointed out that aluminum and iron oxides have high PZC values (usually at pH 8). The high PZC in bentonite clay is an attribute of the presence of aluminum and iron oxide or

Table 2. BET surface, micropore area, external surface area, micropore volume and total pore diameter of magnesite, bentonite clay, and the composite.

	Magnesite	Bentonite	Composite
BET surface area	14.6129	16.01	20.2
Micropore area	2.271	4.92	6
External surface area	12.3419	11.08	14.2
Micropore volume	0.0009	0.0021	0.003
Adsorption average pore diameter (4 V/A by BET)	222.9594	74.07	264

Table 3. Concentration of main exchangeable cations (mg L^{-1}) and calculated cation exchange capacities at pH 5.4 and 7.4 for bentonite clay and the composite.

	Raw bentonite		Composite	
Parameter	pH 5.4	pH 7.4	pH 5.4	pH 7.4
Na	115.2	117.7	120	123
K	3.3	3.7	4	3.9
Ca	57.1	56.2	58.1	57
Mg	86.4	87.9	255	259
CEC (meq 100 g^{-1})	262	265.5	437.1	442.9

hydroxides in the clay matrix (Masindi 2014). The pH_{pzc} value of a material is a reflection of the individual pH_{pzc} values of the components present. Clay and oxide contents increase the pH_{pzc} of the material (Gitari 2014). Mixing bentonite clay with magnesite increases Mg^{2+}, hence leading to an increase in pH_{pzc} for the composite. High PZC of the composite will enhance the efficiency of the material to scavenge anions of arsenic from aqueous media.

Optimization experiments

Several operational parameters were evaluated to establish the optimum condition for the removal of arsenic from the aqueous solution. These were agitation time, dosage, concentration, and pH.

Effect of equilibration time on removal of arsenic

Sorption of arsenic onto the composite with an increase in contact time was investigated (Figure 6). From the first minutes of interaction, there was a drastic increase in sorption

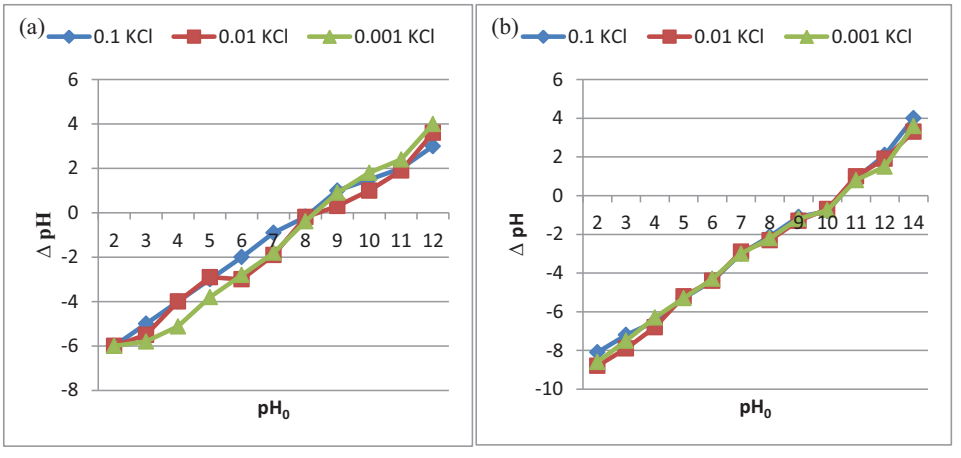

Figure 5. Initial pH (pH_0) and ΔpH of supernatant in pH_{pzc} determination for bentonite clay and the composite.

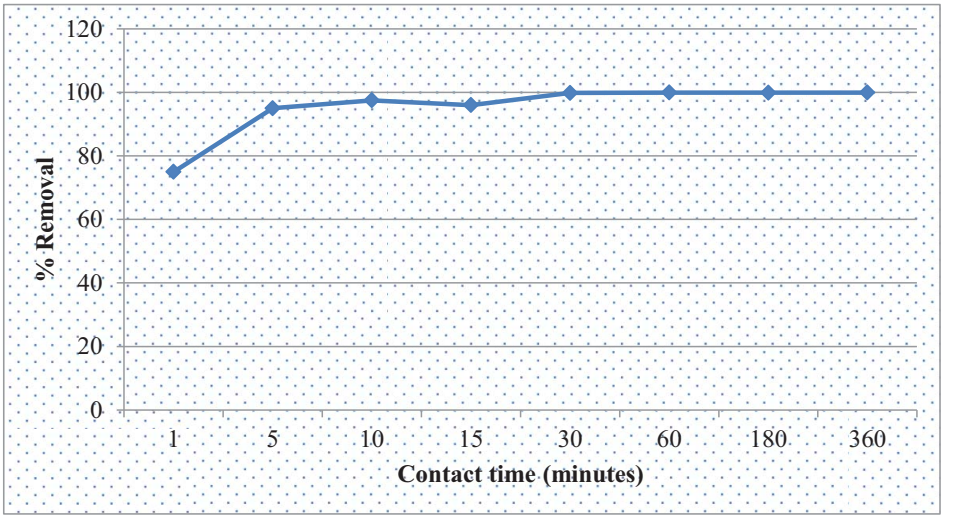

Figure 6. Variation of arsenic concentration with an increase in agitation time (1 g of the composite, 10 mg L^{-1} of arsenic, 250 rpm, and at ambient temperature). Time was varied from 1 to 360 minutes.

capacity of the composite for arsenic. This was observed to increase with an increase in equilibration time. At 30 minutes, the system seems to have approached a steady state since no further change in adsorption was observed. At 30 minutes, the system managed to remove ≈100% of arsenic from the solution. High percentage removal of arsenic may also be attributed to the presence of base cations such as Mg^{2+}, Ca^{2+}, Na^{+}, and K^{+} on the composite matrices. Those base cations will bind with arsenic to form a complex of arsenic. Maximum adsorption of arsenic was observed at 30 minutes of agitation, hence this time was established as the equilibrium reaction time and was applied in subsequent experiments.

Effect of composite dosage on removal of arsenic

The percentage removal of arsenic was observed to increase with an increase in the composite adsorbent dosage (Figure 7). An increase in removal of arsenic with an increase in dosage was attributed to more adsorption sites being available as the dosage increased. Two grams of the composite has provided enough surfaces for adsorption of arsenic from the aqueous solution. This was revealed by the stabilization observed in the percentage removal, hence showing that the composite managed to remove arsenic from the aqueous solution. Close to 100% removal of arsenic was observed at 2 g dosage; hence, this was taken as the optimum dosage and was applied in subsequent experiments.

Effect of arsenic concentration on removal of arsenic

Figure 8 shows that, as the concentration of arsenic increases, the sorption capacity of the composite was gradually decreasing. A decrease in adsorption percentage may be attributed to adsorption surfaces becoming finite as the adsorbate concentration increases. At low concentration, more surfaces are available for adsorption of arsenic and at elevated

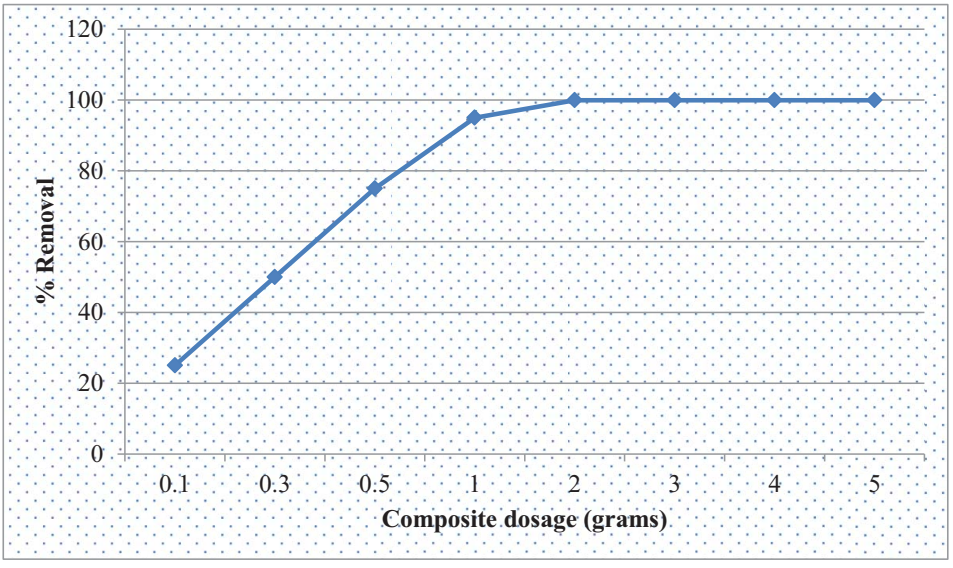

Figure 7. Variation of arsenic concentration with an increase in composite dosage (30 minutes of equilibration, 10 mg L^{-1} of arsenic, 250 rpm, and at ambient temperature). Composite dosages were varied from 0.1 to 5 g.

concentration more surfaces are occupied with arsenic. However, post 20 mg/L of arsenic concentration, the percentage removal of arsenic by the composite was gradually going down. As such, it was concluded that 20 mg L^{-1} will be the optimum concentration of arsenic that can be removed by 2 g of the composite.

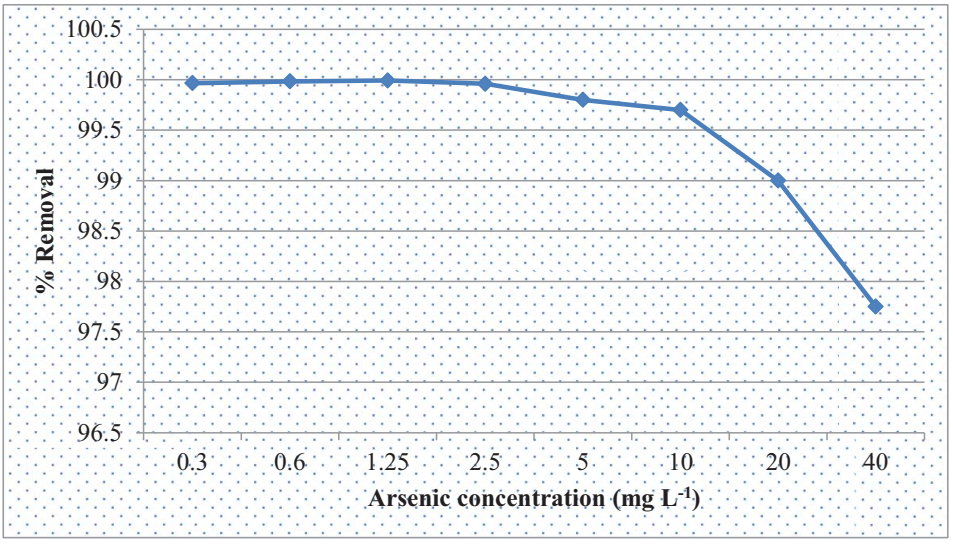

Figure 8. Variation of arsenic concentration with an increase in adsorbate concentration (30 minutes of equilibration, 2 g of the composite, 250 rpm, and at ambient temperature). Arsenic concentrations were varied from 0.3 to 40 mg L^{-1}.

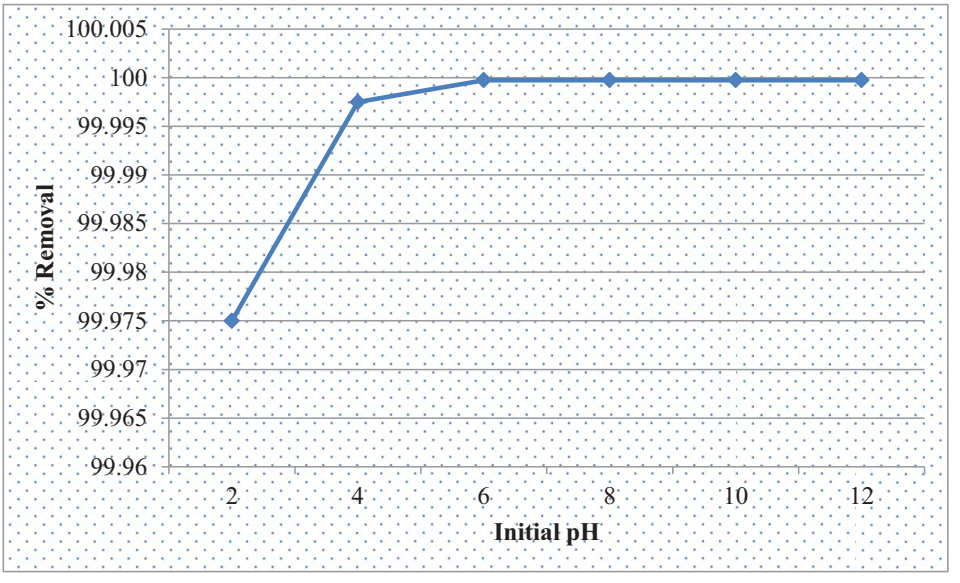

Figure 9. Variation of arsenic concentration with an increase in pH (30 minutes of equilibration, 2 g of the composite, 20 mg L^{-1}, 250 rpm, and at ambient temperature). pH varied from 2 to 12.

Effect of solution pH on removal of arsenic

The amount of arsenic adsorbed depends on the distribution of arsenic species which are mainly controlled by the pH of the solution. Those species mainly compete for adsorption sites on the composite matrices. Due to weathering of the composite, the material release base cations such as Mg^{2+}, Ca^{2+}, Na^{+}, and K^{+}. Those species play an exceptional role in elevating the pH of the counter solution (Table 1). The elevated pH promotes the conversion of As^{3+}/As^{5+} into oxyanion form. At pH > pH_{pzc}, OH^{-} dominates the system, resulting in a charge reversal on the hydroxide surfaces, which leads to electrostatic repulsion between arsenic and surface hydroxyls (generated by accumulation of OH^{-}) (Sparks 1997). Nevertheless, the pH_{pzc} of the composite plays a notable part in adsorption of arsenic species from aqueous solution. The pH_{pzc} of the composite has been established to be 11. For a value above pH_{pzc}, the adsorber surfaces are negatively charged and they are conducive for cation adsorption. For a value below pH_{pzc}, the adsorber surfaces are negatively charged and they are conducive for anion adsorption. Arsenic becomes dominant species at neutral to basic pH. The pH of the solution is an important parameter in determining the adsorption process because it affects solubility of metal ions and concentration of the counter ions on the functional group of the adsorbent. From Figure 9, it is shown that, there is a sharp increase of adsorption from pH 2 to 6, after that the adsorption becomes steady. As pH increases, the composite adsorbs more arsenic onto its matrices since it is rich in basic cations of earth alkali metals (Mg^{2+}, Ca^{2+}, Na^{+}, and K^{+}). When the composite is introduced to an aqueous solution, it rapidly increases the pH of the solution, hence creating conditions which favor the adsorption of arsenic. Moreover, it was concluded that from circumneutral to basic pH condition, the composite will be capable of removing arsenic from aqueous solution.

Table 4. Comparison of adsorption capacities of materials used for removal of arsenic.

Adsorbents	Adsorption capacity (mg g^{-1})	Reference
Al^{3+}-bentonite	2.3	Masindi (2012)
Fe^{3+}-bentonite	2.4	Masindi (2012)
Mg^{+} bent composite	4.0	Present study
Magnesite	5.4	Masindi (2014)
Leonardite	4.5	Chamumui et al. (2014)
Fe_2O_3	4.6	Park et al. (2009)
Fe_2O_4	0.2	Turk, Alp, and Deveci (2010)
$Fe_2O_4 \cdot \gamma Fe_2O_3$	4.9	Chowdhury, Yanful, and Pratt (2010)
CuO nanoparticles	1.1	Pena et al. (2005)
Crystalline TiO_2	37.5	Goswami, Raulb, and Purkaita (2012)
Cross-linked polyethylenimine	1.4	Saad, Cukrowska, and Tutu (2013)

Removal of arsenic at optimized conditions

The removal of arsenic was observed to be high and effective. The composite removed arsenic to below WHO-recommended water quality guidelines. Before the treatment process, the concentration of arsenic was 20 mg L^{-1} and after treatment it was 0.001 mg L^{-1}. The composite removed arsenic from contaminated water to below WHO guidelines of 0.01 mg L^{-1}.

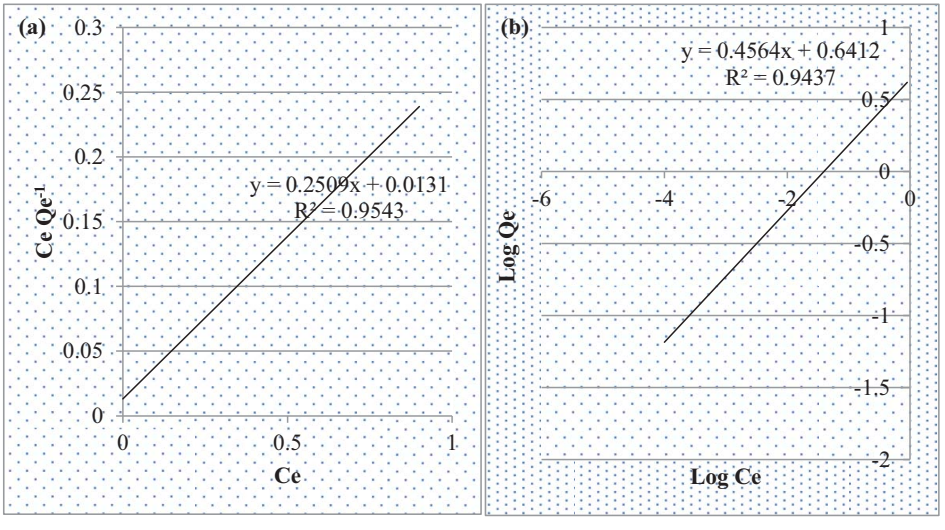

Figure 10. (a and b) The adsorption isotherm models: (a) the Langmuir isotherm model, (b) the Freundlich isotherm model. Reaction conditions: 30 minutes of equilibration, 2 g of the composite, 250 rpm, and at ambient temperature. Arsenic concentrations were varied from 0.3 to 40 mg L^{-1}.

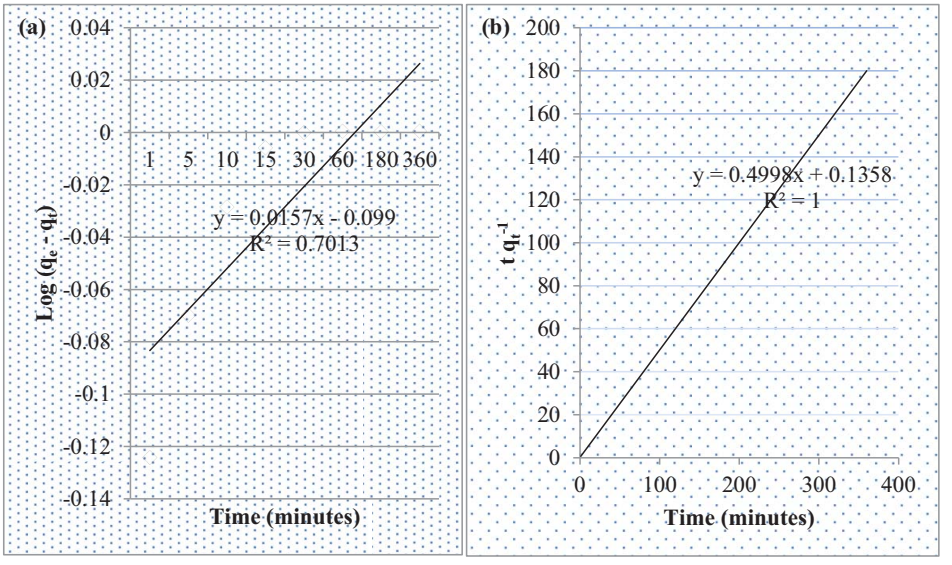

Figure 11. (a and b) The adsorption kinetic models: (a) the pseudo-first order kinetic model, (b) the pseudo-second-order model. Reaction conditions: 1 g of the composite, 10 mg L^{-1} of arsenic, 250 rpm, and at ambient temperature. Time was varied from 1 to 360 minutes.

Comparison of the present study with other adsorbents

To compare the adsorption capacity of the composite with other adsorbents that have been used for arsenic removal, a comparison table is provided (Table 4).

Adsorption isotherm

The results from isotherm modeling suggest that both Langmuir and Freundlich models fit the data better as shown by the correlation coefficient of 0.9543 for Langmuir (Figure 10(a)) and the correlation coefficient of 0.9437 for Freundlich (Figure 10(b)). This result demonstrates adsorption on both homogeneous and heterogeneous surfaces.

Adsorption kinetics

The results from the kinetic models revealed that the data fits well to a pseudo-second-order reaction ($R^2 = 1$) (Figure 11(b)) than pseudo-first-order reaction ($R^2 = 0.7013$) (Figure 11(a)), hence proving that the adsorption of arsenic to the composite is governed by chemisorption.

Conclusions

The study has pointed to the potential of the magnesite−clay composite as an adsorbent for arsenic. Adsorption was found to be high (above 95%) across all pH regimes, an important aspect especially considering that arsenic speciation would change over those pH regimes. The high pH_{pzc} of the composite (around 11) is likely to have contributed to this elevated adsorption capacity. The kinetic study showed that the adsorption of arsenic

onto the composite adsorbent occurred via a chemisorptive mechanism, implying that strong bonds were established between arsenic and adsorptive sites. Isothermic models showed that both the Langmuir and Freundlich isotherms prevailed, suggesting that adsorption could be occurring on both homogeneous and heterogeneous sites.

The composite adsorbent has shown a superior adsorption capacity compared to most of the conventional adsorbents that are used for arsenic removal, making it an attractive alternative to these. The novelty of this work could be viewed in the context of the wide possibilities of application of this composite that range from filter systems to remediate industrial effluent to *in situ* application where the composite can be used as an amendment to soils that have been impacted by arsenic-containing industrial effluent. This latter application can be extended to other situations where arsenic pollution is problematic, for example, in agricultural plots where herbicides and pesticides containing arsenic are often used. The soils in such cases are inadvertently impacted by arsenic, making amendment intervention using this composite, whose components match the soil matrix, possible. Moreover, magnesite and bentonite are cheap and widely available in South Africa, making such a remediation endeavor feasible and cost effective.

Acknowledgments

The authors would like to convey their sincere gratitude to the Research and Innovation Directorate, Department of Ecology and Resource Management, School of Environmental Science, University of Venda, Council of Scientific and Industrial Research (CSIR), Department of Science and Technology and National Research Foundation (DST-NRF), SASOL-Inzalo, and ESKOM-TESP for supporting this project.

References

Agnello, V.N. 2003. “Magnesite.” In *South Africa’s Mineral Industry*, 142−145. Pretoria: Department of Mineral Resource and Energy.

Alloways, B.J. 1995. *Heavy Metals in Soils*. 2nd ed. London: Blackie Academic and Professional.

Aroke, U.O., U.A. El-Nafaty, and O.A. Osha. 2014. “Removal of Oxyanions Contaminants from Wastewater by Sorption onto HDTMA-Br Surface Modified Organo-Kaolinite Clay.” *International Journal of Emerging Technology and Advanced Engineering* 4: 2250−2459.

Bates, M.N., A.H. Smith, and C.H. Rich. 1992. “Arsenic Ingestion and Internal Cancer: A Review.” *America Journal of Epidemiology* 135: 462−467.

Brammer, H., and P. Ravenscroft. 2009. “Arsenic in Groundwater: A Threat to Sustainable Agriculture in South and South-East Asia.” *Environmental International* 35: 647−654.

Bruce, A.M., and S. Goldberg. 1996. “Modelling Arsenate Competitive Adsorption on Kaolinite, Montmorillonite and Illite.” *Clays and Minerals* 44: 609−623.

Chamumui, Y., P. Sooksamiti, W. Naksata, and O. Arqueropanyo. 2014. “Kinetics and Mechanisms of Arsenic Ions Removal by Adsorption on Leornardite Char as Low Cost Adsorbent Materials.” *Journal of the Chilean Chemical Society* 59 (1): 2378−2381.

Chien, C.W.S., H.S. Chen, M. Geethangili, and H.B. Huang. 2012. “Adsorption Characteristics of Aqueous Arsenic (III) and Arsenic (V) in Taiwan Soils.” *International Journal of Applied Science and Engineering* 10 (4): 333−344.

Chowdhury, S.R., E. Yanful, and A. Pratt. 2010. “Arsenic Removal from Aqueous Solutions Mixed Magnetite-Maghemite Nanoparticles.” *Environmental Earth Sciences* 91: 2238−2247.

DWAF (Department of Water Affairs and Forestry). 1996. *South African Water Quality Guidelines*. 2nd ed. Vol. 4 of *Domestic Water Use*. Pretoria, South Africa: DWAF Production.

Gitari, W.M. 2014. “Attenuation of Metals Species in Acidic Solutions using Bentonite Clay: Implication for Acid Mine Drainage Remediation.” *Toxicology and Environmental Chemistry*. doi: 10.1080/02772248.2014.923426

Goh, K.H., T.T. Lim, A. Banas, and Z. Dong. 2010. "Sorption Characteristics and Mechanisms of Oxyanions and Oxyhalides Having Different Molecular Properties on Mg/Al Layered Double Hydroxide Nanoparticles." *Journal of Hazardous Materials* 179 (1−3): 818−827.

Goswami, A., P.K. Raulb, and M.K. Purkaita. 2012. "Arsenic Adsorption Using Copper Oxide (II) Nanoparticles." *Chemical Engineering Research and Design* 90 (9): 1387−1396.

Khan, N.I., G. Owens, D. Bruce, and R. Naidu. 2009. "Human Arsenic Exposure and Risk Assessment at the Landscape Level: A Review." *Environmental Geochemistry and Health* Suppl 1: 143−166. doi: 10.1007/s10653-008-9240-3

Kumar, E., A. Bhatnagar, U. Kumar, and M. Sillanpaa. 2011. "Defluoridation from Aqueous Solution by Nano-alumina: Characterization and Sorption Studies." *Journal of Hazardous Materials* 186: 1042−1049.

Langmuir, D. 1997. *Aqueous Environmental Geochemistry*. Upper Saddle River, NJ: Prentice-Hall.

Lo, I.M.C., K. Yin, and S.C.N. Tang. 2011. "Combining Material Characterization with Single and Multi-oxyanion Adsorption for Mechanistic Study of Chromate Removal by Cationic Hydrogel." *Journal of Environmental Sciences* 23 (6): 1004−1010.

Masindi, V. 2012. "Removal of Oxyanions of As, B, Cr, Mo and Se from Coal Fly Ash Leachates Using Al^{3+}/Fe^{3+} Modified Bentonite Clay." Unpublished MSc thesis.

Masindi, V. 2014. "Remediation of Acid Mine Drainage and Mine Leachates Using a Combination of Magnesite and Bentonite Clay: A Batch Experimental and Geochemical Modelling Approach." Unpublished PhD thesis.

Mishael, G.Y., and N. Bleiman. 2010. "Selenium Removal from Drinking Water by Adsorption to Chitosan−Clay Composites and Oxides: Batch and Columns Tests." *Journal of Hazardous Materials* 183 (1−3): 590−595. doi: 10.1016/j.jhazmat.2010.07.065

Park, H., N.V. Myung, H. Jung, and H. Choi. 2009. "As(V) Remediation Using Electrochemically Synthesized Maghemite Nanoparticles." *Journal of Nanoparticle Research* 11: 1981−1989.

Pena, M.E., G.P. Korfiatis, M. Patel, L. Lippincott, and X. Meng. 2005. "Adsorption of As(V) and As(III) by Nanocrystalline Titanium Dioxide." *Water Research* 39: 2327−2337.

Ramesh, A., H. Hasegawa, T. Maki, and K. Ueda. 2007. "Adsorption of Inorganic and Organic Arsenic from Aqueous Solution by Polymeric Al/Fe Modified Montmorillonite." *Separation and Purification Technology* 56: 90−100.

Saad, D.M., E.M. Cukrowska, and H. Tutu. 2013. "Functionalisation of Cross-linked Polyethylenimine for the Removal of As from Mining Wastewater." *Water SA* 39 (2): 257−264.

Singh, D., and S. Bhati. 2012. "Adsorption of Cr (VI) Metal Ion from Aqueous Solution on Low Cost Adsorbent." *Biointerface Research in Applied Chemistry* 2 (2): 284−290.

Sparks, D.L. 1997. *Environmental Soil Chemistry*. 2nd ed. Amsterdam: Academic Press.

Tseng, W.P. 1977. "Effects and Dose−Response Relationships of Skin Cancer and Black Foot Disease with Arsenic." *Environmental Health Perspective* 19: 109−119.

Turk, T., I. Alp, and H. Deveci. 2010. "Adsorption of As(V) from Water Using Nanomagnetite." *Journal of Environmental Engineering* 136: 399−404.

WHO (World Health Organization). 2006. *Guidelines for Drinking-Water Quality [Electronic Resource]: Incorporating First Addendum*. Vol. 1. *Recommendations*. 3rd ed. *Electronic Version for the Web. 1. Potable Water − Standards. 2. Water − Standards. 3. Water Quality − Standards. 4. Guidelines. I. Title*. Geneva: WHO Press.

Yang, W.J., K.W. Park, and C.Y. Lee. 2011. "Removal of Anionic Metal by Amino-organoclay for Water Treatment." *Journal of Hazardous Materials* 190: 652−658.

Zachara, J.M, C.E. Cowan, R.L. Schmidt, and C.C. Ainsworth. 1998. "Chromate Adsorption by Kaolinite." *Clays and Minerals* 36: 317−326.